Carbohydrate Polymers 88 (2012) 809–819

Contents lists available at SciVerse ScienceDirect

Carbohydrate Polymers

journal homepage: www.elsevier.com/locate/carbpol

Acceleration of wound healing in diabetic rats by layered hydrogel dressing

Yen-Hsien Lee[a], Jung-Jhih Chang[b], Ming-Chien Yang[a,b,*], Chiang-Ting Chien[c,**], Wen-Fu Lai[d]

[a] Graduate Institute of Applied Science and Technology, National Taiwan University of Science and Technology, Taipei 106, Taiwan, ROC
[b] Department of Materials Science and Engineering, National Taiwan University of Science and Technology, Taipei 106, Taiwan, ROC
[c] Department of Medical Research, National Taiwan University Hospital and National Taiwan University College of Medicine, Taipei 100, Taiwan, ROC
[d] Graduate Institute of Medical Sciences, Taipei Medical University, Taipei 110, Taiwan, ROC

ARTICLE INFO

Article history:
Received 4 November 2011
Received in revised form
10 December 2011
Accepted 24 December 2011
Available online 18 January 2012

Keywords:
Wound healing
Alginate
Chitosan
Poly(γ-glutamic acid)
Rat model

ABSTRACT

In this study, a novel layered hydrogel composing of alginate (AL), chitosan (CS), and poly(γ-glutamic acid) (PGA) was prepared. The resulting hydrogel was characterized, including the swelling ratio, water vapor transmission rate, the release of Ca^{2+} and blood coagulation activity. *In vitro* evaluation of cell migration and proliferation were carried out on electric cell-substrate impedance sensing (ECIS). Effect of the hydrogels on wound healing was examined in type 1 diabetic rat model induced by streptozotoxin (STZ). After grafting to full-thickness wounds in diabetic rats, AL–CS–PGA exhibited higher rate of wound healing than conventional AL hydrogels. Epithelialization and collagen deposition were examined histologically. Hydroxyproline levels also were assessed in the wound skin. The results indicated AL–CS–PGA treated wounds showed increased collagen regeneration and epithelialization. Therefore AL–CS–PGA can improve wound healing of diabetic rat models comparing to conventional AL wound dressing.

1. Introduction

Wound healing is a complex biological process including blood coagulation, inflammation, fibroplasia, collagen deposition, and wound contraction (Gurtner, Werner, Barrandon, & Longaker, 2008). The impaired healing seen in diabetic human is also seen in diabetic animal models, where poor wound healing is found in genetically diabetic mice and also in streptozotocin-induced diabetic rats (Darby, Bisucci, Hewitson, & MacLellan, 1997). Such animals thus provide good model systems as well as considering changes seen in diabetes in general, both in humans and animal models, that may in turn contribute to ulcer formation (Blakytny & Jude, 2006).

The principal functions of wound dressings are to remove wound exudates, to prevent the entry of harmful bacteria into the wound, and to promote the establishment of the best milieu for natural healing (Boateng, Matthews, Stevens, & Eccleston, 2008; Ovington, 2007). At present, high quality wound dressings are designed to create a moist environment to promote healing.

Sodium alginate (AL) is a natural linear polysaccharide consisting of 1,4-linked β-D-mannuronic acid (M) and α-L-guluronic acid (G) units. Alginate exhibits excellent biocompatibility, non-toxicity, non-immunogenicity, biodegradability, and can be easily gelled with divalent cations such as calcium ion (George & Abraham, 2006). Alginate wound dressing is fabricated by introducing calcium ions into sodium alginate solution, and has been used clinically to absorb excess exudates to maintain an appropriate moist environment at the wound surface (Qin, 2008).

Chitosan (CS), a polycation biopolymer, is a nontoxic, biocompatible, and biodegradable polysaccharide derived from naturally occurring chitin (Berger, Reist, Mayer, Felt, & Gurny, 2004; Murakami et al., 2010). Positively charged CS is soluble in acidic aqueous solution below pH 6, while generally insoluble in neutral conditions and most organic solvents. Chitosan has many useful and advantageous properties such as hemostatic activity, wound healing ability, reducing scars, and antimicrobial activity, as well as inhibition of a wide variety of bacteria (Kim et al., 2008; Muzzarelli, 2009a). Therefore, CS has been investigated for using as wound dressing (Ribeiro et al., 2009).

Poly(γ-glutamic acid) (PGA) is a hydrophilic, nontoxic, edible, and biodegradable polymer (Huang & Yang, 2010). PGA is a linear homo-polyamide composed of D- and L-glutamic acid units connected by amide linkages between α-amino and γ-carboxyl groups. Each repeating unit of PGA contains one α-carboxyl group, and that shows specific affinity for some biomaterials, hence it is successfully utilized in biomedical field such as drug carrier and wound dressing (Wang, Su, Chen, & Chen, 2009; Yu, 2007).

* Corresponding author at: Department of Materials Science and Engineering, National Taiwan University of Science and Technology, Taipei 106, Taiwan, ROC. Tel.: +886 2 2737 6528; fax: +886 2 2737 6544.
** Corresponding author. Tel.: +886 2 2312 3456x65720; fax: +886 2 2394 7927.
E-mail addresses: myang@mail.ntust.edu.tw (M.-C. Yang), ctchien@ntuh.gov.tw (C.-T. Chien).

0144-8617/$ – see front matter © 2012 Elsevier Ltd. All rights reserved.
doi:10.1016/j.carbpol.2011.12.045

In the literature, polyanion–polycation complexes formed from alginate and chitosan have been investigated and their drug release properties have been studied (George & Abraham, 2006). Iwasaki et al. indicated that the alginate-based chitosan hybrid polymer fibers promoted favorable biological responses of seeded chondrocytes including enhancing cell attachment and proliferation (Iwasaki et al., 2004). Moreover, Hsieh et al. reported that the PGA can be well mixed with chitosan to fabricate both dense and porous PGA/chitosan composite matrices (Hsieh, Tsai, Wang, Chang, & Hsieh, 2005). In our laboratory, we successfully prepared alginate/Ca-PGA hydrogels film as wound dressing and drug release carrier (Huang & Yang, 2010).

Recently, several multilayered wound dressings were developed to promote wound healing. Griffiths et al. developed a multilayered wound dressing comprising an adhesive layer and an absorbent layer for highly exuding wounds located on areas of the body that require a high degree of flexibility from the dressing (Griffiths, Pritchard, Jacques, Bishop, & Lydon, 2004; Griffiths, Pritchard, Jacques, Bishop, & Lydon, 2010). Bishop et al. prepared a multilayered wound dressing for wounds producing high levels of exudate. Their dressings are consisting of a transmission layer, an absorbent core, and a wound contacting layer, which transmits exudate to the absorbent core, while the absorbent core and wound contacting layer limiting the lateral extend of exudate in the dressing to the region of the wound (Bishop, Griffiths, Linnane, Lydon, & Shaw, 2010). In accordance with this trend, a layered hydrogel consisting of PGA, AL, and CS was developed in our laboratory (Lee, Chang, Lai, Yang, & Chien, 2011). The base layer was composed of AL to provide mechanical strength, while the top layer was composed of PGA and CS to serve as absorbent.

In this study, the feasibility of using this layered hydrogel as functional wound dressings for healing wounds was investigated. The physical properties (*i.e.* swelling ratio, water vapor transmission rate, and durability) of the hydrogel film were measured. Additionally, the hemocompatibility of hydrogel was evaluated based on blood coagulation times and complete blood count (CBC). The effect of these hydrogels on cell migration was assessed *in vitro* using electric cell-substrate impedance sensing (ECIS) device. Furthermore, the *in vivo* performance of this hydrogel for wound healing was evaluated histologically using diabetic rat models.

2. Experimental

2.1. Materials

Calcium PGA (Ca-PGA, Mw 1 MD) was provided by Vedan Enterprise Corporation, Taiwan. Sodium alginate (Mw 22 kD) and chitosan (Mw 20 kD) were purchased from Acros (USA). Reagents for activated partial thrombin time (APTT), and prothrombin time (PT) were purchased from Dade Behring Inc., USA. Seasorb™ soft dressing (alginate dressing) was purchased from Coloplast, Denmark. Platelet poor plasma (PPP) was provided by the Blood Center in Taipei. Zoletil was purchased from Virbac Laboratories, France. Streptozotocin (STZ) was purchased from Sigma, USA.

2.2. Preparation of hydrogel

A 1.5 wt% alginate (AL) solution was preparation by dissolving sodium alginate powder in deionized (DI) water at 25 °C for 24 h under stirring to form a homogeneous solution. Chitosan (CS) powder was dissolved in 5 wt% aqueous acetic acid at 25 °C under stirring for 24 h to form a homogeneous solution of 1 wt%. Calcium PGA powder was dissolved in DI water at 25 °C under stirring for 2 h to form a homogeneous solution of 3 wt%.

Afterwards, 20 ml of AL solution were cast onto a glass plate and air-dried at 25 °C for 1 day. Then 20 ml of the CS solution was poured over the dry sodium alginate film and air-dried at 25 °C for 1 day. Finally, 20 ml of the Ca-PGA solution was poured over the dry AL–CS film to form a hydrogel film. The resulting hydrogel was labeled as AL–CS–PGA. For comparison, dry sodium alginate film was soaked in either 10 wt% $CaCl_2$ or 3 wt% Ca-PGA aqueous solution. The resulting hydrogel was labeled as AL–$CaCl_2$ and AL–PGA, respectively. Then these hydrogel films were dried at 60 °C for 1 day in an oven. Fig. 1 depicts the gelation mechanisms of these three types of hydrogel used in this work.

2.3. Determination of swelling ratio

The swelling ratio of hydrogel was defined as the weight ratio of absorbed water to dry hydrogel. The dried sample (2 cm × 2 cm) was immersed in a sealed tube containing excess amount of normal saline (0.9 wt% NaCl, pH 7.4) at ambient temperature and weighed at specific time points. The weight of wet sample was measured after blotting the surface water. The swelling ratio (SR%) of each sample was calculated as follows:

$$\mathrm{SR\%} = \frac{W_{\mathrm{wet}} - W_{\mathrm{dry}}}{W_{\mathrm{dry}}} \times 100$$

where W_{wet} is the weight of the sample at equilibrium swelling and W_{dry} is the weight of the dry sample. Each swelling experiment was repeated six times and the average value was recorded.

2.4. Water vapor transmission rate (WVTR)

The water vapor transmission tests were conducted according to JIS 1099A standard. A circular piece of the specimen was fastened over the top of a cup of 7 cm in diameter containing 50 g of $CaCl_2$. The cup was then placed in an incubator at 90 ± 5% RH at 40 ± 2 °C. The water vapor transmission rate (WVTR) was calculated as follows:

$$\mathrm{WVTR} = \frac{W_2 - W_1}{S} \times 24\,(\mathrm{kg/m^2/day})$$

where W_1 and W_2 are the weights of the whole cup at the 1st and 2nd hour, respectively, and S is the transmitting area of the specimen. The diffusion coefficient of water vapor through the hydrogel film is calculated as follows:

$$D = \frac{JRT}{0.9P} \times d\,(\mathrm{m^2/s})$$

where d is the thickness of the hydrogel film, P is the saturated water vapor pressure, which is 7370 Pa at 40 °C, and J is the molar flux of water vapor, defined as

$$J = \frac{\mathrm{WVTR}}{(18\,\mathrm{g/mol})(86400\,\mathrm{s/day})}(\mathrm{mol/m^2/s})$$

2.5. Determination of blood coagulation activity

The *in vitro* coagulation times, including, activated partial thromboplastin time (APTT), and prothrombin time (PT) were determined using an automated blood coagulation analyzer (CA-50, Sysmex, Japan). APTT is a measure of the integrity of the intrinsic pathway, and is performed by mixing blood with kaolin (which provides an electronegative surface), a phospholipid, and calcium (Minors, 2007). Briefly, a piece of dry sample (1 cm × 1 cm) was put in an Eppendorf tube, and pre-swelled with 0.35 ml of platelet-poor plasma (PPP). Then 50 μl of the plasma were pipetted into a reaction tube and set it into the detector. Then, 50 μl of the APTT assay

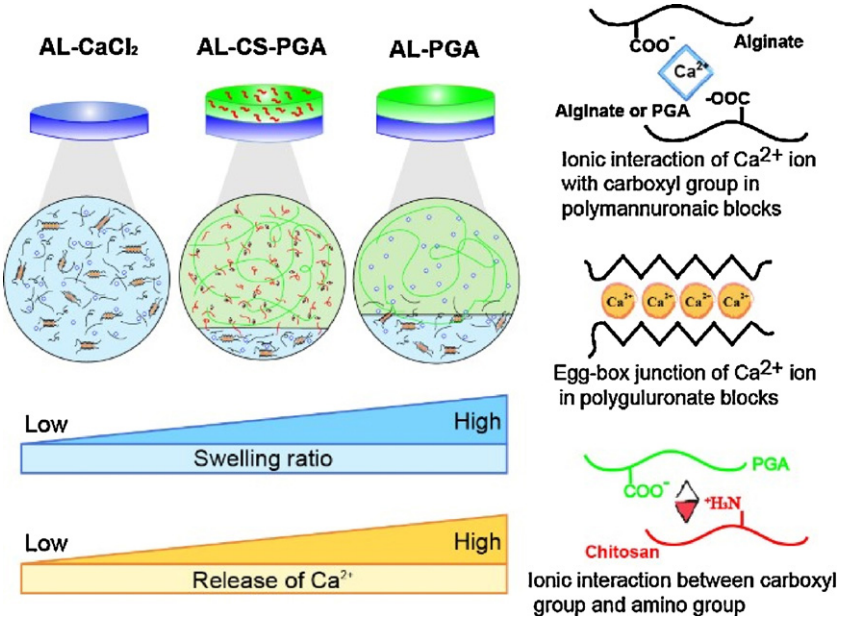

Fig. 1. The gelation mechanisms of three types of hydrogel studied in this work.

reagent was added after 1 min of incubation. Finally, 50 μl of $CaCl_2$ solutions were added after 3 min of incubation.

PT is a measure of the integrity of the extrinsic pathway and is performed by adding blood to tissue thromboplastin derived from brain tissue and calcium. After contacting the sample for 30 min, 50 μl of plasma were pipetted to the reaction tube and set it into the detector. Then 100 μl of the PT assay reagent was added after 3 min of incubation.

2.6. Hematological parameters

A piece of sample (1 cm × 1 cm) was incubated with 2 ml of fresh rat blood at 37 °C for 30 min. Hematological parameters were determined by Lezen Reference Laboratory Center in Taipei. These parameters included white blood cell (WBC) count, red blood cell (RBC) count, and platelet (PLt) count.

2.7. Electric cell-substrate impedance sensing (ECIS)

Electric cell-substrate impedance sensing (ECIS) is a technology which is not only capable of producing quantitative data, but is also able to monitor experiments in real-time (Giaever & Keese, 1984). ECIS measures the interaction between cells and the substrate to which they are attached *via* gold-film electrodes placed on the bottom of culture dishes. Through these electrodes, the ability of the cell monolayer to impede a non-invasive AC signal can be measured. As cultured cells attach and spread onto the electrodes, the current is impeded proportional to the number of attached cells, the number of tight junctions between cells and the shortness in distance between the cells and the substratum (McCoy & Wang, 2005).

In this work, we used the ECIS Model 800 (Applied BioPhysics, Troy, USA) with ECIS electrode array chip (8W1E, Applied BioPhysics, Troy, USA) to monitor cell behavior. Each array chip is comprised of eight wells. The surface of each well contains an active gold microelectrode (250 μm in diameter) for detecting the current flow through the medium. The array holder was placed in a standard cell culture incubator (37 °C, in 5% CO_2). The array chips were equilibrated with 200 μl of DMEM in the incubator at cell culture conditions overnight. Then, 1×10^5 fibroblast L929 cells were seeded to each well containing 200 μl of either Dulbecco's Modified Eagle Medium (DMEM) or hydrogel extracts. During the incubation, cell attachment and spreading were followed by means of impedance (Giaever & Keese, 1984). Data were collected continuously for 70 h at 15 kHz and the sampling interval was 150 s.

To understand the migration of the wounded cells, microscopic observations of the cells on the active electrode were made before and after wounding.

2.8. In vitro release of Ca^{2+}

A piece of dry sample (10 cm × 10 cm) was weighted before immersing in 50 ml of DMEM solution supplemented with 10% fetal bovine serum at 25 °C for 24 h in a shaker at 50 rpm. At appropriate time intervals, an aliquot was withdrawn and treated with the calcium detecting kit (HI93752A&B, Hanna Instruments, USA). The concentration of calcium was determined from the reading using a photometer (HI83200, Hanna Instruments, USA). All the measurements were repeated three times.

2.9. Release of polymers from hydrogels in DMEM

To investigate the stability of each component in the hydrogels, alginate was labeled with DAPI (AL–DAPI), chitosan was labeled with RdB (CS–RdB), and PGA was labeled with FITC (PGA–FITC) according to our previous work (Lee et al., 2011). Briefly, AL–DAPI was prepared by mixing 1.76% AL with 0.1 mg/ml DAPI and 0.2 mg/ml EDC at 4 °C for 1 d. CS–RdB was prepared by mixing 1% CS with 0.5 mg/ml RdB and 0.2 mg/ml EDC at 4 °C for 1 day. PGA–FITC was prepared by mixing 3% PGA with 0.4 mg/ml FITC, 0.2 mg/ml EDC and 0.2 mg/ml lysine at 4 °C for 1 day. The residual free dyes were then dialyzed off in DI water for 4 weeks. These labeled polymers were mixed with neat polymers to prepare hydrogels as described in previous section.

Afterwards, pieces of dry sample (10 cm × 10 cm) were weighted before immersing in 50 ml of DMEM solution supplemented with 10% fetal bovine serum at 25 °C for 24 h in a shaker at 50 rpm. At specified time intervals, the samples were withdrawn and the fluorescein count of fluorescence-labeled polymers released was determined using an ELISA reader (Wallac 1420

Victor^2 multilabel counter, EG&G Wallac, USA). The release of fluorescence-labeled polymers was calculated as follows:

$$\text{Release}(\%) = \frac{\text{weight of fluorescence-labeled polymer in DMEM}}{\text{weight of dry sample}} \times 100$$

2.10. Induction of diabetes mellitus rats

All the animal experiments were conducted with the ethical approval of National Taiwan University Hospital Animal Center. Female Wistar rats, weighing 220 ± 20 g were used for this experiment. All rats were housed at a constant temperature and humidity in a room with an artificial 12 h light/dark cycle and allowed free access to food and water.

Diabetes was induced by a single 65 mg/kg intravenous injection of STZ, a toxin specific for insulin-producing cells, in saline-sodium citrate buffer. Blood glucose levels were measured using an acute glucometer. 21 days after STZ injection, animals with blood glucose levels above 300 mg/dl were defined as diabetic and used in the study (Qiu, Kwon, & Kamiyama, 2007).

2.11. Permeation of hydrogel components through rat skin

The permeation of each component was performed using DM rat skin. The rats were anesthetized with Zoletil and hair on the back of the rat was shaved using an electric clipper. The fluorescence-labeled hydrogel was immersing in 50 ml of PBS at 25 °C for 0.5 h. Afterwards, the wet hydrogel was applied onto the skin of the rat's back. After 24 h, the hydrogels were carefully removed and full thickness biopsies from the center of the treated area were taken with a new biopsy punch. The biopsies were rinsed thrice with PBS, wiped dry, and frozen on dry ice. A piece of tissue was cut out from biopsy sample, embedded in optimal cutting temperature compound (OCT), and cut with a cryostat. Fluorescence-labeled polymer in the skin sections was visualized using a confocal microscope (LSM 510 META, Carl Zeiss Inc., USA) (Batheja, Sheihet, Kohn, Singer, & Michniak-Kohn, 2011).

2.12. Full-thickness skin wound preparation and various treatments

Diabetic animals with confirmed glucose levels above 300 mg/dl were anesthetized with Zoletil. The dorsal skin of the animals was shaved and cleaned with iodine solution, and a full-thickness skin wound (approximately 1 cm × × 1 cm) was created.

Wound closure was measured at 0, 3, 7, 10, 14, and 21 day after wounding. Animals were euthanized at 7, 14 and 21 day and the wound samples and adjacent normal skin were harvested and fixed in 10% paraformaldehyde for histological examination or snap-frozen in liquid nitrogen and stored at −80 °C for further analysis.

2.13. Wound healing rate

The percentage of wound closure was calculated as follows by using the initial and final area drawn on glass slides during the experiments.

The wound contraction was calculated as follows (Yates et al., 2007):

$$\%\text{Wound contraction} = \frac{A_0 - A_t}{A_0} \times 100$$

where A_0 is the original wound area and A_t is the area of wound at the time of biopsy on days 0, 3, 7, 10, 14 and 21 days accordingly.

2.14. Hydroxyproline analysis

Collagen is an important structural protein of the body being of particular importance in connective tissues by providing their durability. Proline, seldom appearing in other protein, is the major and relatively constant amino acid in collagen. Through the determination of hydroxyproline, the content of collagen could be detected so as to evaluate the wound-healing abilities (Baoyong, Lian, Denglong, & Min, 2010; Edwards & O'Brien, 1980).

Wound tissues stored at −80 °C were dried to a constant weight and hydrolyzed in 6 M HCl for 16 h at 120 °C. After neutralized with NaOH, 0.1 ml of the solution were added to 2 ml of acetate–citrate buffer (1.2% sodium acetate trihydrate, 5% citric acid, 12% sodium acetate and 3.4% sodium hydroxide, pH 4–9). Then 0.5 ml of 0.05 M chloramine-T were added to 1 ml of each sample, after which the samples were incubated for 15 min at 25 °C, followed by the addition of 0.5 ml of 15% perchloric acid and 0.5 ml of 15% 4-dimethyl aminobenzaldehyde in 2-propanol. After incubation at 60 °C for 15 min, each sample was transferred to an ELISA reader and the absorbance was read at 550 nm (Wallac 1420 Victor^2 multilabel counter, EG&G Wallac, USA).

2.15. Histological analysis

Tissue was collected, treated with formaldehyde (10%), and embedded in paraffin. Then the samples were cut into sections of 4 μm in thickness by cryomicrotome (Leica RM 2145, Nussloch, Germany). After tissue sections were dewaxed and rehydrated conventionally, sections were stained with Masson's Trichrome Staining kit (HT15, Sigma, USA). By this staining, the collagen would be stained as blue, while keratin would be stained as red. The stained samples were then examined using an optical microscope.

2.16. Immunohistochemistry examination

Loricrin is the main component of the epidermal cornified envelope. Human loricrin is initially deposited in the granular layer of the epidermis in keratohyalin granules and is intermixed with profilaggrin. Newborn rodent epidermis contains morphologically distinct profilaggrin and loricrin granules (Candi, Schmidt, & Melino, 2005). Differentiation of the neo-epidermis was studied by immunohistology using loricrin as late differentiation marker (Candi et al., 2005; Shih & Van, 2001).

After tissue sections were dewaxed and rehydrated conventionally, sections were incubated with 3% H_2O_2 for 30 min. The slides were washed with phosphate buffer solution (PBS, pH 7.4) twice. The sections were blocked with 5% BSA in tris buffer solution (TBS) for 20 min. After the redundant liquid was discarded, the sections were incubated with loricrin antibody (Abcam, Cambridge, UK) at 4 °C overnight. After slides were washed with PBS, the slides were incubated with rabbit secondary antibody for 1 h, followed by incubating with streptavidin–HRP for 20 min. The antibody binding sites were visualized by incubation with DAB–H_2O_2 solution. The slides were stained for 1 min with hematoxylin and then dehydrated with sequential ethanol for microscope observation.

3. Results and discussion

3.1. Swelling behavior of hydrogels

Swelling behavior is one of the most important properties of hydrogels for wound dressing application. The water sorption

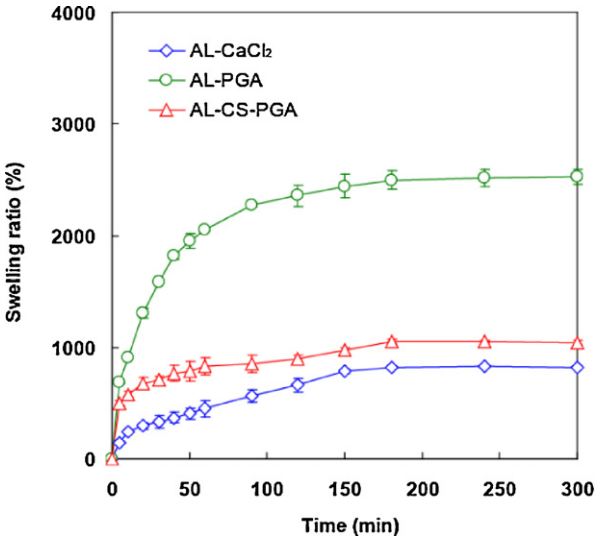

Fig. 2. Swelling behavior of AL–$CaCl_2$, AL–PGA, and AL–CS–PGA hydrogels ($n = 6$).

ability of hydrogel should be adequate for the removal of wound exudates.

Fig. 2 shows the swelling ratios of the AL–$CaCl_2$, AL–PGA, and AL–CS–PGA hydrogels in normal saline for 5 h. The equilibrium swelling ratios of AL–PGA, and AL–CS–PGA were about 3.1 and 1.3 times of that of AL–$CaCl_2$, respectively. In this work, PGA is the major component of the AL–PGA and AL–CS–PGA hydrogels. The AL–PGA was composed of 87% of PGA and 13% of AL. On the other hand, the AL–CS–PGA was constituted of 81% of PGA, 12% of AL, and 7% of CS. Because PGA is highly hygroscopic (Shih & Van, 2001), the swelling ratio of AL–PGA and AL–CS–PGA were higher than that of AL–$CaCl_2$. Between these two layered hydrogels, the swelling ratio of AL–CS–PGA was lower than that of AL–PGA, because CS can interact with PGA, hence reducing the interaction between water and PGA. Hsieh et al. reported the swelling ratio of PGA/CS composite decreased with the increase of CS content (Hsieh et al., 2005). This is similar to our observation.

3.2. Water vapor transmission rate

The water vapor transmission rate (WVTR) is one of the most important parameter for wound dressing. In the literature, Lamke et al. reported that the evaporative water loss rate (*i.e.* WVTR) from the skin has been found to vary considerably depending on the wound type and healing stage, ranging from 0.204 kg/m^2/day for normal skin to 0.279 kg/m^2/day and as much as 5.138 kg/m^2/day for first-degree burns and granulating wounds, respectively (Lamke, Nilsson, & Reithner, 1977). The high WVTR may lead to the total dehydration of the wound surface (Balakrishnan, Mohanty, Umashankar, & Jayakrishnan, 2005), whereas a low WVTR may lead to maceration of healthy surrounding tissue and buildup of a back pressure and pain to the patient. Queen et al. suggested that a WVTR of 2–2.5 kg/m^2/day will be sufficient to give moisture and prevent wound dehydration (Queen, Gaylor, Evans, Courtney, & Reid, 1987).

Table 1
The water vapor transmission rate and the diffusion coefficient of vapor through the hydrogel film (mean ± SD) ($n = 3$).

Sample	WVTR (kg/m^2/day)	J (mol/m^2/s)	d (cm)	D (m^2/s)
AL–$CaCl_2$	2.32 ± 0.25	0.00149	0.03 ± 0.01	1.75×10^{-7}
AL–CS–PGA	2.97 ± 0.11	0.0019	0.042 ± 0.01	3.14×10^{-7}
AL–PGA	3.11 ± 0.17	0.002	0.05 ± 0	3.93×10^{-7}

Table 1 lists the WVTR and diffusion coefficient (D) of the hydrogels. As shown in Table 1, the WVTR for AL–PGA, and AL–CS–PGA were about 1.34 and 1.28 times of that of AL–$CaCl_2$, respectively. This can be explained by the mobility of molecular chains. Alginate chains can be crosslinked by Ca^{2+}, hence are less mobile than uncrosslinked PGA chains. Therefore, the diffusion coefficient of water in AL–$CaCl_2$ was about 44% of that of AL–PGA. The presence of CS can restrict the mobility of PGA chains due to ionic interaction. Therefore the diffusion coefficient of AL–CS–PGA was about 80% than that of AL–PGA. In this work, the values of WVTR of the hydrogels were close to the ideal range of the recommended evaporative water loss rate of injured skin.

3.3. Blood coagulation

In humans, normal hemostasis depends on the complex interaction of clotting of blood plasma and aggregation of platelets through the release of clotting factors (Lansdown, 2002). On contacting directly with foreign material, blood could activate the immune complement system and trigger the blood plasma coagulation cascade, resulting in harmful effects such as acute inflammatory reaction and thrombus formation. The blood coagulation cascade involves an intrinsic pathway, an extrinsic pathway, and a common pathway (Gorbet & Sefton, 2004; Minors, 2007). The blood compatibility of these hydrogels is evaluated with APTT and PT for the intrinsic and common pathways, respectively (Chang, Lin, Yang, & Chien, 2009).

Table 2 shows that the values of APTT of AL–$CaCl_2$, AL–PGA, and AL–CS–PGA were 25.7 ± 1.2, 27.5 ± 1.2, and 26.5 ± 1.5 s, respectively, which were about 76% of that of the plasma (35.1 ± 0.3 s). In addition, the values of PT of AL–$CaCl_2$, AL–PGA, and AL–CS–PGA were 14.3 ± 0.1, 12.8 ± 0.4, and 11.6 ± 0.7 s, respectively. The PT of AL–PGA, and AL–CS–PGA were about 87% of that of the plasma (14.8 ± 0.1 s). The shortening of APTT and PT can be attributed to the release of Ca^{2+} from the hydrogels.

In the literature, calcium ions (coagulation factor IV), when released from alginate dressings into the wound, play a physiological role assisting the clotting mechanism during the first stage of wound healing (Boateng et al., 2008). Calcium ions can promote the synthesis and release of factors VII, IX, and X, and the conversion of prothrombin to thrombin (Lansdown, 2002). In this work, all these hydrogels contained calcium. Thus these hydrogels would promote blood coagulation.

3.4. The complete blood cell count (CBC) assay

The complete blood cell (CBC) count assay is a common blood test that evaluates the major types of cells in the blood includes red blood cells (RBC), white blood cells (WBC), and platelets. If the RBC count is low, the body may not be getting the oxygen it needs, that led to anemia. The white blood cells (WBC) test measures the relative numbers of the different kinds of WBCs in the blood. An abnormal WBC count may indicate an infection, inflammation, or other stress in the body. Additionally, hematocrit (Hct) test measures the volume percentage of RBCs in the whole blood and is a measure of both the number and the size of RBCs. Hemoglobin (Hgb) test measures the amount of hemoglobin in the blood and is a good measure of the blood's ability to carry oxygen throughout the body.

Table 2 summarizes the results of hematological analysis of rat for the samples. As shown in Table 2, the values of RBC and Hgb were close to that of the control. The values of WBC for AL–CS–PGA, AL–$CaCl_2$, and AL–PGA were 81.1%, 84.6%, and 80.2%, respectively, of that of the control. The adhesion of WBC onto biomaterials has been reported in the literatures (Grooteman et al., 1997) although the mechanism is still not fully clear (Gorbet & Sefton, 2004). In

Table 2
Evaluation of hemocompatibility based on complete blood count (CBC) test, coagulation time and platelet adhesion on hydrogel film (mean ± SD) ($n = 6$).

Parameters	Control (rat blood)	AL–$CaCl_2$	AL–PGA	AL–CS–PGA
RBC (10^{12} l^{-1})	8.5 ± 0	8.4 ± 0	8.3 ± 0	8.3 ± 0
WBC (10^9 l^{-1})	5.7 ± 0.2	4.9 ± 0.5	4.6 ± 0.3	4.6 ± 0.1
Hgb (g/dl)	14.2 ± 0.2	14 ± 0.1	13.6 ± 0.1	13.9 ± 0.1
Hct (%)	41.7 ± 0.2	40.7 ± 0.1	40.2 ± 0.1	41.5 ± 1.7
Platelet count (10^6 ml^{-1})	736 ± 40	638 ± 6	611 ± 14	633 ± 54
Platelet adhesion (10^6 cm^{-2})	–	48.8 ± 1.2	62.3 ± 2.9	51.3 ± 8.7
APTT coagulation time (s)	35.1 ± 0.3	25.7 ± 1.2	27.5 ± 1.2	26.5 ± 1.5
PT coagulation time (s)	14.8 ± 0	14.3 ± 0.1	12.8 ± 0.4	11.6 ± 0.7

Abbreviations: RBC: red blood cells, WBC: white blood cells, Hgb: hemoglobin, and Hct: hematocrit.

addition to the adhesion of WBC, the adhesion of platelets was also observed.

The platelet is a specialized adhesive cell in the blood that plays a key role in the normal hemostatic process through its ability to firmly adhere to subendothelial matrix proteins and to other activated platelets at sites of vascular injury (Jackson, 2007; Nesbitt et al., 2003). Hence, platelet adhesion is an important test for the evaluation of the blood compatibility of the biomaterials. Table 2 shows that the number of platelets adhering on the samples. Among these three samples, AL–$CaCl_2$ exhibited the minimum adhesion of PLts (48.8×10^6 cm^{-2}), while those of AL–PGA and AL–CS–PGA were 62.3×10^6 cm^{-2} and 51.3×10^6 cm^{-2}, respectively. This trend agrees with the trend of Ca^{2+} release discussed in later section, because Ca^{2+} is a central and common second messenger downstream of most signaling pathways in platelets (Varga-Szabo, Braun, & Nieswandt, 2009).

3.5. Electric cell-substrate impedance sensing (ECIS)

Fig. 3A shows the microscopic observations of the cells before and after wounding on an ECIS chip. Immediate after wounding, the cells on the circular electrode became flattened with less defined cell boundaries, while the cells in the surrounding area remained the same. This indicates the death of the cells on the electrode. After the electrocution, cells migrated gradually from the surrounding onto the electrode, as indicated by the arrows.

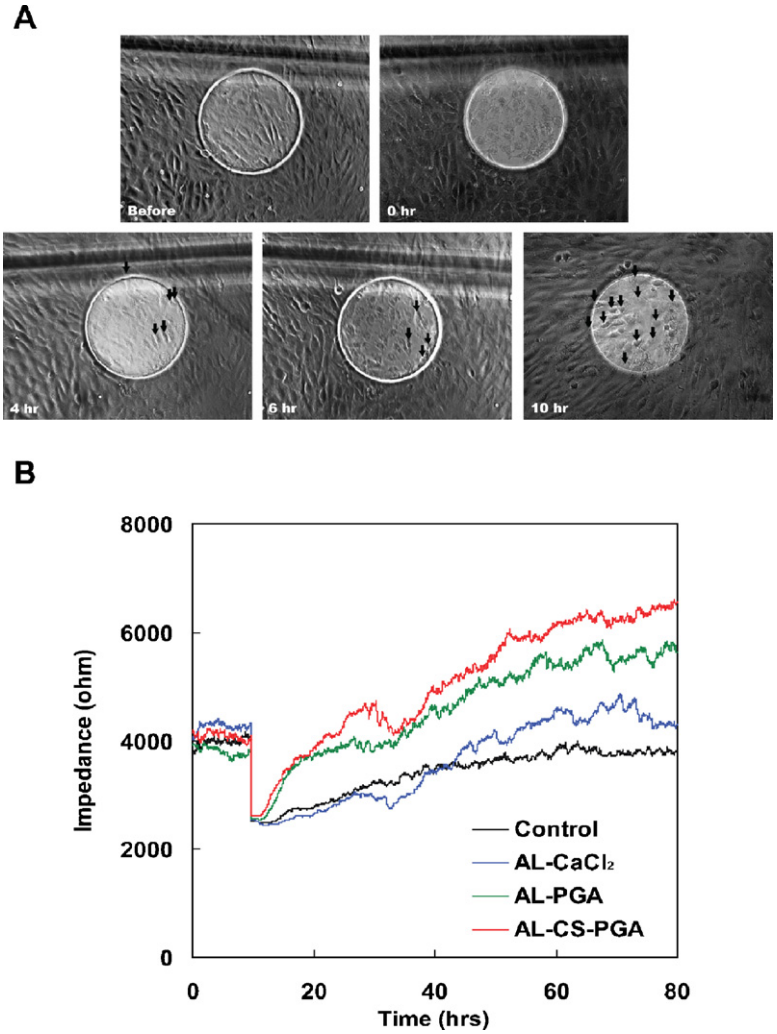

Fig. 3. Wound healing measurement by ECIS. (A) Microscopic observations of the cells before and after wounding on an ECIS chip. The arrows indicated the cells migrated into the electrode. (B) The variation of the impedance before and after wounding. 1×10^5 cells/well were seeded into ECIS 8W1E arrays.

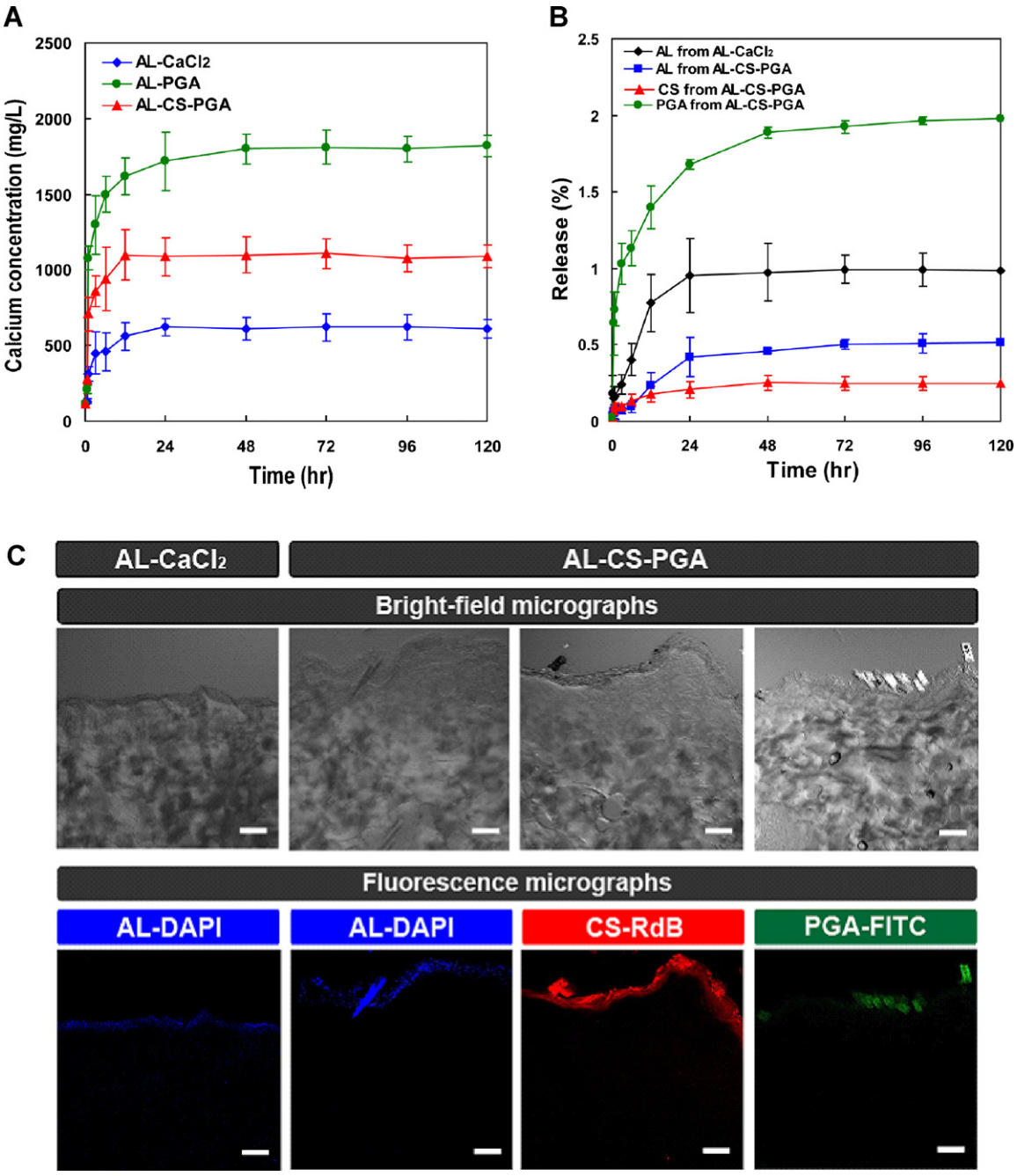

Fig. 4. (A) The release of calcium ion from hydrogel in DMEM for 5 days ($n = 6$). (B) The release of each hydrogel component in DMEM for 5 days ($n = 6$). (C) Cross-sectional micrographs obtained after topical application of hydrogel for 5 days (scale bar = 50 μm).

Fig. 3B shows the ECIS for wound healing measurement. The increase in the impedance was due to the migration of cells from the perimeter to the cell-free electrode. The fluctuation in the curves was due to the movement of the cells. When fibroblasts attached and spread to the detecting electrode surface, a significant increase in the impedance will be observed (Xiao, Lachance, Sunahara, & Luong, 2002; Xiao & Luong, 2003).

Fig. 3B shows that all four curves increased after electrocuting. Among them, those cells cultured with the extracts from AL–PGA and AL–CS–PGA exhibited higher rate of increase in the impedance than those cells cultured with extract from AL–$CaCl_2$ and the control. This suggests that the presence of PGA may be able to promote the activity of L929 fibroblasts. In the literature, PGA has been reported to be favorable for the proliferation of L929 fibroblast (Tsao et al., 2010). Hiseh et al. reported that the rat osteosarcoma cells proliferated well on the PGA/chitosan composite biomaterial surface (Hsieh et al., 2005). In our previous study, we found AL–$CaCl_2$ and AL–PGA were nontoxicity for L929 (Huang & Yang, 2010; Lee et al., 2011). In addition, AL–PGA can also promote the proliferation of L929. Our present results agreed with these literatures.

3.6. Calcium ions release of hydrogels in DMEM

Because calcium can affect the behavior of fibroblast L929, the release of calcium ions from these hydrogels to DMEM was determined. In fact, DMEM contains various monovalent and divalent ions including Na^+, K^+, and Ca^{2+}. Fig. 4A shows that Ca^{2+} ions were indeed released from hydrogels into DMEM. The order of the release rate of Ca^{2+} in DMEM was AL–PGA > AL–CS–PGA > AL–$CaCl_2$. The

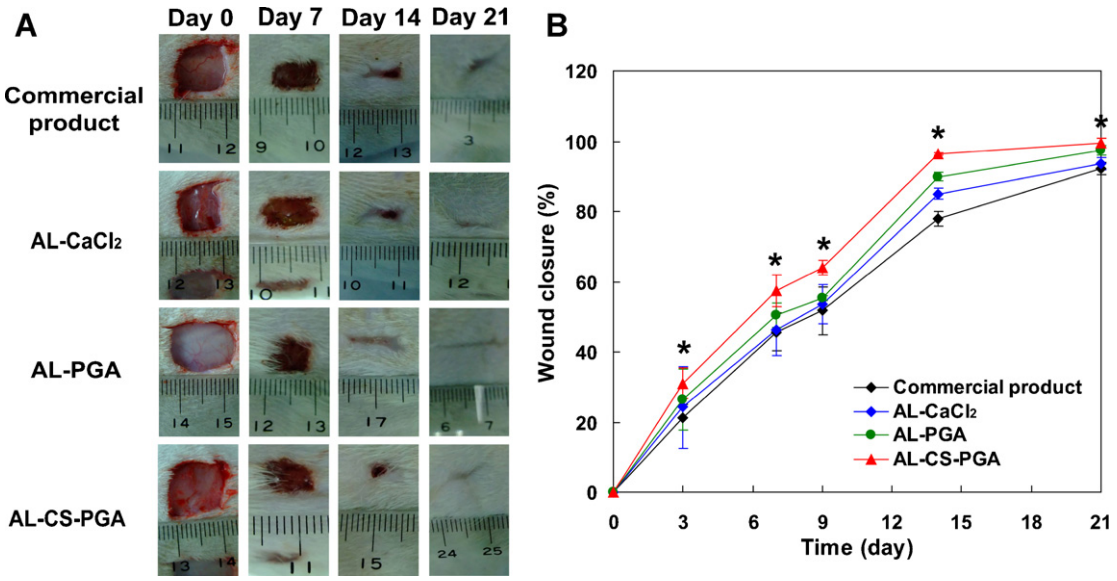

Fig. 5. (A) Photographs of wound treated with commercial product, AL–$CaCl_2$, AL–PGA, or AL–CS–PGA at 7, 14 and 21 days. In the cases of AL–CS–PGA and AL–PGA, the PGA layer is contacting the wound. (B) Wound closure with commercial product, AL–$CaCl_2$, AL–PGA, or AL–CS–PGA. Values are mean ± SD for each group. $^*p < 0.05$.

release of Ca^{2+} seemed to be in a two stage. Rapid release occurred within the first 1 h. This phenomenon was similar to the previous study (Bajpai & Sharma, 2004).

The release of Ca^{2+} from the hydrogel is governed by the diffusion of calcium ions inside the hydrogel. More swollen hydrogel leads to faster diffusion since the diffusion of ions is faster in water than in polymer matrix. Thus the release rate of Ca^{2+} was in the same order of the swelling ratio. Although the composition was similar, the release rate of Ca^{2+} of AL–PGA was faster than AL–CS–PGA by about 70%. This indicates that the introduction of CS can reduce the release of calcium in DMEM from the sample, since CS can interact with PGA to form a denser hydrogel. In the case of AL–$CaCl_2$, because a large portion of Ca^{2+} was locked in the egg-box structure, leading to a lower swelling ratio and less free calcium ions to be released, thus the release rate was the lowest among these three samples.

Even though calcium ions were released from the hydrogels, the curves in Fig. 3B show that L929 can still migrate to the wound (the electrode). This suggests that in this case, Ca^{2+} would not prohibit the healing of the wound, although the concentration was much higher than the original value in the DMEM.

3.7. Stability test of hydrogel

Fig. 4B shows that the time-course of the release of hydrogel components in DMEM for 5 day. The release of AL from AL–DAPI–$CaCl_2$ was much faster than that from AL–DAPI–CS–PGA. After 5 day, AL–$CaCl_2$ lost about 1% of AL, while AL–CS–PGA lost only 0.5% of AL. This can be attributed to the exchange of Ca^{2+} with Na^+ from DMEM, leading to the disintegration of AL–$CaCl_2$ (McCoy & Wang, 2005). In addition, the AL–CS–PGA was composed of 81% of PGA, 12% of AL, and 7% of CS (Lee et al., 2011). Therefore, in the case of AL–CS–PGA, the order of the release rate is PGA > AL > CS.

3.8. Penetration of hydrogel components through rat skin

Fig. 4C shows representative fluorescent microscope images of vertically cross-sectioned skin after topical application of various hydrogels. After 24 h, the penetration of all hydrogel components (AL, CS, and PGA) was not observable. This is because all these components are polymers, and skin is a barrier of these polymers. Thus the penetration of hydrogel components would occur only through the wound on the skin.

3.9. Wound closure in rats treated with hydrogel

In open wound-healing tests, full-thickness rectangular wounds were made on the back of each rat. Fig. 5A shows representative animals from each group (commercial product, AL–$CaCl_2$, AL–PGA, and AL–CS–PGA) at 0, 7, 14 and 21 d after grafting. Among these dressings, the wound area treated by AL–CS–PGA seemed to be smaller than other samples at 7th and 14th days after wounding. Fig. 5B depicts the wound closure rates of wounds treated with those hydrogels. After 3, 7, 9, 14, and 21 day, a significant increase ($p < 0.05$) in the rate of wound closure in the AL–CS–PGA when comparing to the commercial product. Comparing with other groups, the wound treated with AL–CS–PGA exhibited the fastest wound closure.

Previous study by Park et al. indicated that accelerated wound healing of acute wounds has been observed with chitosan treatment (Park, Clark, Lichtensteiger, Jamison, & Johnson, 2009). They further showed that chitosan attracted neutrophils without inducing the excessive inflammation that would otherwise be expected due to elevated levels of neutrophils. Moreover, Tsao et al. showed that animal studies revealed that wounds treated with the CS/PGA PECs healed significantly faster than wounds without treatment (Tsao et al., 2011). Furthermore, inflammatory phenomena were suppressed and reduced, and re-epithelialization was activated in wounds treated with the CS/PGA PECs. Therefore, the fast wound closure of AL–CS–PGA may be attributed to the chitosan in the hydrogel.

3.10. Histological analysis and hydroxyproline analysis

Since collagen formation is a critical step for the wound healing, the skin tissue was stained with Masson's trichrome kit that can highlight the collagen remodeling and maturation. Fig. 6A shows the histological analysis of granulated tissue from treated group at different days. The results indicate that AL–CS–PGA-treated wounds exhibited abundant mature and compact collagen comparing with other treatments. This agrees with the results from the hydroxyproline measurement shown in Fig. 6B.

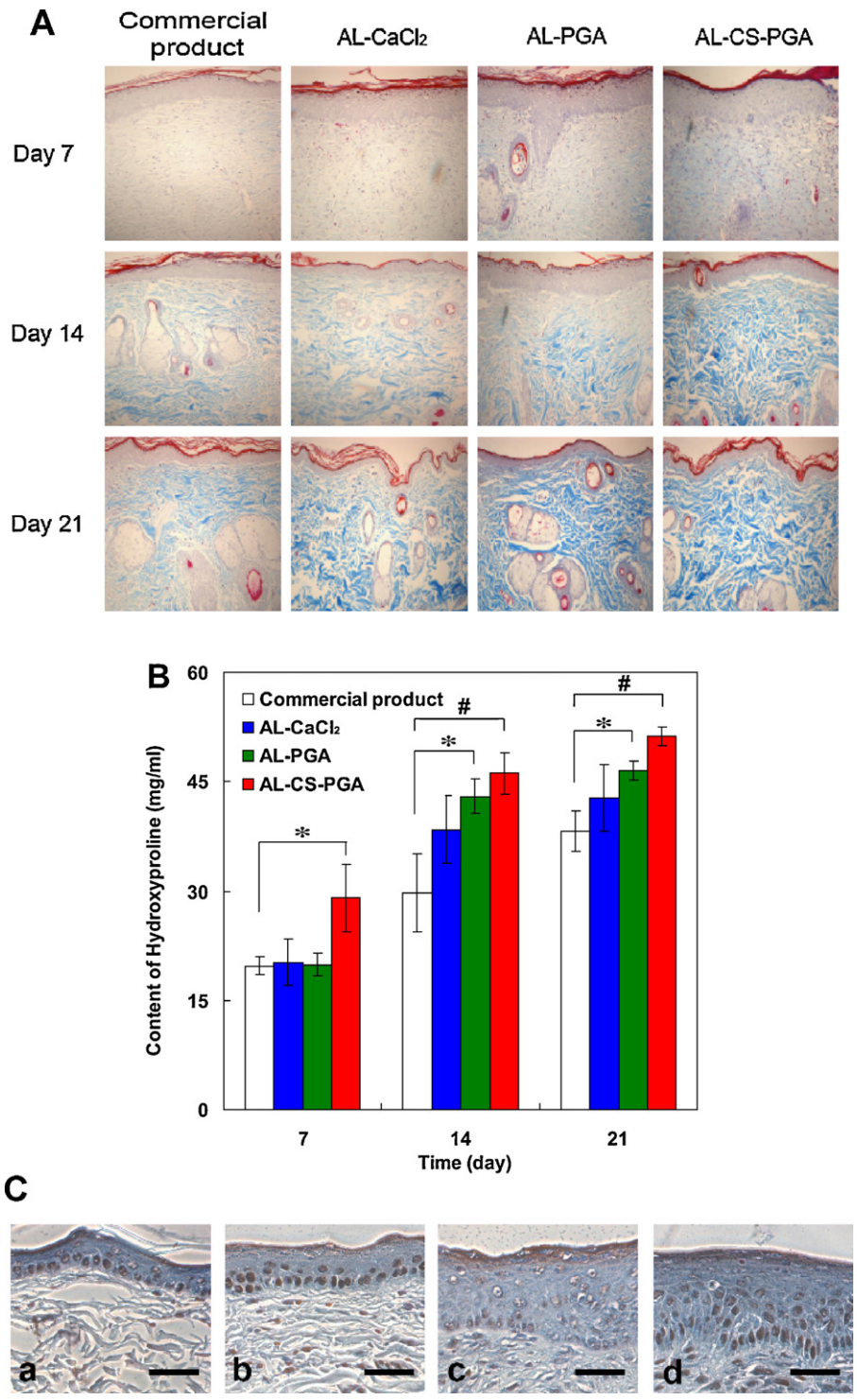

Fig. 6. (A) Masson's trichrome staining for collagen. Tissue sections from wound skin of various groups were stained with Masson's trichrome staining for collagen formation (the magnification was 200×). (B) Hydroxyproline levels in wound tissue during wound healing. Values are mean ± SD, $n = 6$ for each group. $^{*}p < 0.05$, $^{\#}p < 0.01$. (C) Immunohistochemical staining of loricrin (scale bar = 100 μm) on day 14. The representative images from groups of (a) commercial product, (b) AL–$CaCl_2$, (c) AL–PGA and (d) AL–CS–PGA. Loricrin was stained brown with DAB and other tissues were stained blue with hematoxyline.

As shown in Fig. 6B, on the 7, 14 and 21 day, the content of hydroxyproline for the AL–CS–PGA group was the highest among these four groups, suggesting that AL–CS–PGA could promote collagen synthesis in the injury wound. This indicates good regeneration of wounded skin in the AL–CS–PGA groups. This may be attributed to the presence of chitosan.

Chitosan has the ability to foster adequate granulation tissue formation accompanied by angiogenesis and regular deposition of thin collagen fibers, a property that further enhances correct repair of dermal-epidermal lesions (Muzzarelli, 2009b; Muzzarelli, Mattioli-Belmonte, Pugnaloni, & Biagini, 1999; Muzzarelli et al., 2007; Shi et al., 2006). Ueno et al. reported that chitosan accelerates the

secretion of type III collagen and results in the increase of granulation in wound healing in dogs (Ueno et al., 1999). Ringler et al. also reported the supply of oxygen and vitamin C was increased by chitosan administration. Oxygen is required for hydroxylation of proline and lysine residues in the polypeptide chains assembled in the cytoplasm of the fibroblast. Without enough oxygen in the extracellular space, hydroxyproline is not formed in the helical procollagen molecule (Ringler, 1997). The results here suggest that the treatment with AL–CS–PGA may be good for collagen proliferation and hence accelerate the wound healing.

3.11. Immunohistochemistry examination

Epidermal differentiation begins with the migration of keratinocytes from the basal layer, and ends with the formation of the cornified layer (the stratum corneum), which is providing physical resistance and acting as a water barrier (Michel, Schmidt, Shroot, & Reichert, 1988; Strelkov, Herrmann, & Aebi, 2003). Loricrin is the main component of the epidermal cornified envelope, and comprises 70–85% of the total protein mass of the cornified layer (Candi et al., 1995; Kalinin, Marekov, & Steinert, 2001; Steinert, Kartasova, & Marekov, 1998; Steinert & Marekov, 1995).

Fig. 6C shows the results of immunohistochemical staining of tissue at the 14th day. Normally, loricrin is expressed as a thin band in stratum corneum. The expressed region of loricrin would extend to the whole layer of stratum granulosum in line with epidermal thickening. Comparing these four images, we observed that loricrin was highly expressed in AL–PGA and AL–CS–PGA groups, suggesting that PGA may facilitate the expression of loricrin, an indication of later differentiation of epidermis (Candi et al., 2005). Furthermore, the loricrin band for AL–CS–PGA group was slightly thicker than that for AL–PGA group. This may be attributed to the presence of CS, which is known to favor the re-epilization in wounds (Howling et al., 2001; Naseema, Padayatti, & Paulose, 1995; Okamoto et al., 1992, 1995). Therefore AL–CS–PGA can accelerate wound healing comparing to other wound dressings in this study.

4. Conclusion

In the present study, an AL–CS–PGA hydrogel with layer structure was prepared for the application of wound dressing. As a wound dressing, this hydrogel can absorb 1000% of water and provide a WVTR of about 3 kg/m^2-day. The results from animal test using diabetic rat models indicated that AL–CS–PGA hydrogel can be used as wound dressing that can accelerate wound healing. This multifunctional hydrogel exhibited hemostatic, and promoted cell migration and collagen synthesis. The immunochemical staining of loricrin showed that AL–CS–PGA hydrogel can facilitate re-epilization. Therefore, such a layered hydrogel of AL–CS–PGA would be applicable for wound dressing.

Acknowledgements

The authors would like to thank the National Science Council of Taiwan, Republic of China, for financially supporting this research under grant NSC-99-2120-M-038-001. The authors would also like to thank National Taiwan University Hospital for providing grant NTUH 100-S1661.

Appendix A. Supplementary data

Supplementary data associated with this article can be found, in the online version, at doi:10.1016/j.carbpol.2011.12.045.

References

Bajpai, S. K., & Sharma, S. (2004). Investigation of swelling/degradation behaviour of alginate beads crosslinked with Ca^{2+} and Ba^{2+} ions. *Reactive and Functional Polymers*, *59*, 129–140.

Balakrishnan, B., Mohanty, M., Umashankar, P. R., & Jayakrishnan, A. (2005). Evaluation of an in situ forming hydrogel wound dressing based on oxidized alginate and gelatin. *Biomaterials*, *26*, 6335–6342.

Baoyong, L., Lian, Z., Denglong, C., & Min, L. (2010). Evaluation of a new type of wound dressing made from recombinant spider silk protein using rat models. *Burns*, *36*, 891–896.

Batheja, P., Sheihet, L., Kohn, J., Singer, A. J., & Michniak-Kohn, B. (2011). Topical drug delivery by a polymeric nanosphere gel: Formulation optimization and in vitro and in vivo skin distribution studies. *Journal Controlled Release*, *149*, 159–167.

Berger, J., Reist, M., Mayer, J. M., Felt, O., & Gurny, R. (2004). Structure and interactions in chitosan hydrogels formed by complexation or aggregation for biomedical applications. *European Journal of Pharmaceutics and Biopharmaceutics*, *57*, 35–52.

Bishop, S. M., Griffiths, B., Linnane, P. G., Lydon, M. J., Shaw, H. (2010). Multi-layered wound dressing. *US Patent Office*, Pat. No. 7 759 537 B2.

Blakytny, R., & Jude, E. (2006). The molecular biology of chronic wounds and delayed healing in diabetes. *Diabetic Medicine*, *23*, 594–608.

Boateng, J. S., Matthews, K. H., Stevens, H. N., & Eccleston, G. M. (2008). Wound healing dressings and drug delivery system: A review. *Journal of Pharmaceutical Sciences*, *97*, 2892–2923.

Candi, E., Melino, G., Mei, G., Tarcsa, E., Chung, S. I., Marekov, L. N., et al. (1995). Biochemical, structural, and transglutaminase substrate properties of human loricrin, the major epidermal cornified cell envelope protein. *Journal of Biological Chemistry*, *270*, 26382–26390.

Candi, E., Schmidt, R., & Melino, G. (2005). The cornified envelope: A model of cell death in the skin. *Nature Reviews Molecular Cell Biology*, *6*, 328–340.

Chang, J. J., Lin, P. J., Yang, M. C., & Chien, C. T. (2009). Removal of lipopolysaccharide and reactive oxygen species using sialic acid immobilized polysulfone dialyzer. *Advanced Polymer Technology*, *20*, 871–877.

Darby, I. A., Bisucci, T., Hewitson, T. D., & MacLellan, D. G. (1997). Apoptosis is increased in a model of diabetes-impaired wound healing in genetically diabetic mice. *The International Journal of Biochemistry & Cell Biology*, *29*, 191–200.

Edwards, C. A., & O'Brien, W. D. (1980). Modified assay for determination of hydroxyproline in a tissue hydrolyzate. *Clinica Chimica Acta*, *104*, 161–167.

George, M., & Abraham, T. E. (2006). Polyionic hydrocolloids for the intestinal delivery of protein drugs: Alginate and chitosan—a review. *Journal of Controlled Release*, *114*, 1–14.

Giaever, I., & Keese, C. R. (1984). Monitoring fibroblast behavior in tissue culture with an applied electric field. *Proceedings of the National Academy of Sciences*, *81*, 3761–3764.

Gorbet, M. B., & Sefton, M. V. (2004). Biomaterial-associated thrombosis: Roles of coagulation factors, complement, platelets and leukocytes. *Biomaterials*, *25*, 5681–5703.

Griffiths, B., Pritchard, D. C., Jacques, E., Bishop, S. M., & Lydon, M. J. (2004). Multi-layered wound dressing. *US Patent Office*, Pat. No. 6 793 645 B2.

Griffiths, B., Pritchard, D. C., Jacques, E., Bishop, S. M., & Lydon, M. J. (2010). Multi-layered wound dressing. *US Patent Office*, Pat. No. 7 803 980 B2.

Grooteman, M. P., Bos, J. C., van Houte, A. J., van Limbeek, J., Schoorl, M., & Nubé, M. J. (1997). Mechanisms of intra-dialyser granulocyte activation: A sequential dialyser elution study. *Nephrology Dialysis Transplantation*, *12*, 492–499.

Gurtner, G. C., Werner, S., Barrandon, Y., & Longaker, M. T. (2008). Wound repair and regeneration. *Nature*, *453*, 314–321.

Howling, G. I., Dettmar, P. W., Goddard, P. A., Hampson, F. C., Dornish, M., & Wood, E. J. (2001). The effect of chitin and chitosan on the proliferation of human skin fibroblasts and keratinocytes in vitro. *Biomaterials*, *22*, 2959–2966.

Hsieh, C. Y., Tsai, S. P., Wang, D. M., Chang, Y. N., & Hsieh, H. J. (2005). Preparation of γ-PGA/chitosan composite tissue engineering matrices. *Biomaterials*, *26*, 5617–5623.

Huang, M. H., & Yang, M. C. (2010). Swelling and biocompatibility of sodium alginate/poly(γ-glutamic acid) hydrogels. *Advanced Polymer Technology*, *21*, 561–567.

Iwasaki, N., Yamane, S. T., Majima, T., Kasahara, Y., Minami, A., Harada, K., et al. (2004). Feasibility of polysaccharide hybrid materials for scaffolds in cartilage tissue engineering: Evaluation of chondrocyte adhesion to polyion complex fibers prepared from alginate and chitosan. *Biomacromolecules*, *5*, 828–833.

Jackson, S. P. (2007). The growing complexity of platelet aggregation. *Blood*, *109*, 5087–5095.

Kalinin, A., Marekov, L. N., & Steinert, P. M. (2001). Assembly of the epidermal cornified cell envelope. *Journal of Cell Science*, *114*, 3069–3070.

Kim, I. Y., Seo, S. J., Moon, H. S., Yoo, M. K., Park, I. Y., Kim, B. C., et al. (2008). Chitosan and its derivatives for tissue engineering applications. *Biotechnology Advances*, *26*, 1–21.

Lamke, L. O., Nilsson, G. E., & Reithner, H. L. (1977). The evaporative water loss from burns and the water–vapour permeability of grafts and artificial membranes used in the treatment of burns. *Burns*, *3*, 159–165.

Lansdown, A. B. (2002). Calcium: A potential central regulator in wound healing in the skin. *Wound Repair and Regeneration*, *10*, 271–285.

Lee, Y. H., Chang, J. J., Lai, W. F., Yang, M. C., & Chien, C. T. (2011). Layered hydrogel of poly(γ-glutamic acid), sodium alginate, and chitosan: Fluorescence observation of structure and cytocompatibility. *Colloids and Surfaces B: Biointerfaces*, *86*, 409–413.

McCoy, M. H., & Wang, E. (2005). Use of electric cell-substrate impedance sensing as a tool for quantifying cytopathic effect in influenza A virus infected MDCK cells in real-time. *Journal of Virological Methods*, *130*, 157–161.
Michel, S., Schmidt, R., Shroot, B., & Reichert, U. (1988). Morphological and biochemical characterization of the cornified envelopes from human epidermal keratinocytes of different origin. *Journal of Investigative Dermatology*, *91*, 11–15.
Minors, D. S. (2007). Haemostasis, blood platelets and coagulation. *Anaesthesia and Intensive Care Medicine*, *8*, 214–216.
Murakami, K., Aoki, H., Nakamura, S., Nakamura, S. I., Takikawa, M., Hanzawa, M., et al. (2010). Hydrogel blends of chitin/chitosan, fucoidan and alginate as healing-impaired wound dressings. *Biomaterials*, *31*, 83–90.
Muzzarelli, R. A. A. (2009a). Genipin-crosslinked chitosan hydrogels as biomedical and pharmaceutical aids. *Carbohydrate Polymers*, *77*, 1–9.
Muzzarelli, R. A. A. (2009b). Chitins and chitosans for the repair of wounded skin, nerve, cartilage and bone. *Carbohydrate Polymers*, *76*, 167–182.
Muzzarelli, R. A. A., Mattioli-Belmonte, M., Pugnaloni, A., & Biagini, G. (1999). Biochemistry, histology and clinical uses of chitins and chitosans in wound healing. In P. Jollès, & R. A. A. Muzzarelli (Eds.), *Chitin and chitinases* (pp. 251–264). Basel: Birkhauser Verlag.
Muzzarelli, R. A. A., Morganti, P., Morganti, G., Palombo, P., Palombo, M., Biagini, G., et al. (2007). Chitin nanofibrils/chitosan glycolate composites as wound medicaments. *Carbohydrate Polymers*, *70*, 274–284.
Naseema, A., Padayatti, P. S., & Paulose, C. S. (1995). Mechanism of wound healing induced by chitosan in streptozotocin diabetic rats. *Current Science*, *69*, 461–464.
Nesbitt, W. S., Giuliano, S., Kulkarni, S., Dopheide, S. M., Harper, I. S., & Jackson, S. P. (2003). Intercellular calcium communication regulates platelet aggregation and thrombus growth. *Journal of Cell Biology*, *160*, 1151–1161.
Okamoto, Y., Minami, S., Matsuhashi, A., Sashiwa, H., Saimoto, H., Shigemasa, Y., et al. (1992). Application of chitin and chitosan in small animals. In C. J. Brine, P. A. Sanford, & J. P. Zikakis (Eds.), *Advanced in chitin and chitosan* (pp. 70–78). New York: Elsevier.
Okamoto, Y., Shibazaki, K., Minami, S., Matsuhashi, A., Tanioka, S., & Shigemasa, Y. (1995). Evaluation of chitin and chitosan in open wound healing in dogs. *Journal of Veterinary Medical Science*, *57*, 851–854.
Ovington, L. G. (2007). Advances in wound dressings. *Clinics in Dermatology*, *25*, 33–38.
Park, C. J., Clark, S. G., Lichtensteiger, C. A., Jamison, R. D., & Johnson, A. J. (2009). Accelerated wound closure of pressure ulcers in aged mice by chitosan scaffolds with and without bFGF. *Acta Biomaterialia*, *5*, 1926–1936.
Qin, Y. (2008). The preparation and characterization of fiber reinforced alginate hydrogel. *Journal of Applied Polymer Science*, *108*, 2756–2761.
Qiu, Z., Kwon, A. H., & Kamiyama, Y. (2007). Effects of plasma fibronectin on the healing of full-thickness skin wounds in streptozotocin-induced diabetic rats. *Journal of Surgical Research*, *138*, 64–70.
Queen, D., Gaylor, J. D., Evans, J. H., Courtney, J. M., & Reid, W. H. (1987). The preclinical evaluation of the water vapour transmission rate through burn wound dressings. *Biomaterials*, *8*, 367–371.
Ribeiro, M. P., Espiga, A., Silva, D., Baptista, P., Henriques, J., Ferreira, C., et al. (2009). Development of a new chitosan hydrogel for wound dressing. *Wound Repair and Regeneration*, *17*, 817–824.
Ringler, D. J. (1997). Inflammation and repair. In T. C. Jones, R. D. Hunt, & N. W. King (Eds.), *Veterinary Pathology* (6th ed., pp. 113–158). Baltimore: Williams & Wilkins.
Shi, C. M., Zhu, Y., Ran, X., Wang, M., Su, Y., & Cheng, T. (2006). Therapeutic potential of chitosan and its derivatives in regenerative medicine. *Journal of Surgical Research*, *133*, 185–192.
Shih, I. L., & Van, Y. T. (2001). The production of poly-(γ-glutamic acid) from microorganisms and its various applications. *Bioresource Technology*, *79*, 207–225.
Steinert, P. M., Kartasova, T., & Marekov, L. N. (1998). Biochemical evidence that small proline-rich proteins and trichohyalin function in epithelia by modulation of the biomechanical properties of their cornified cell envelopes. *Journal of Biological Chemistry*, *273*, 11758–11769.
Steinert, P. M., & Marekov, L. N. (1995). The proteins elafin, filaggrin, keratin intermediate filaments, loricrin, and small proline-rich proteins 1 and 2 are isodipeptide cross-linked components of the human epidermal cornified cell envelope. *Journal of Biological Chemistry*, *270*, 17702–17711.
Strelkov, S. V., Herrmann, H., & Aebi, U. (2003). Molecular architecture of intermediate filaments. *BioEssays*, *25*, 243–251.
Tsao, C. T., Chang, C. H., Lin, Y. Y., Wu, M. F., Wang, J. L., Han, J. L., et al. (2010). Antibacterial activity and biocompatibility of a chitosan–γ-poly(glutamic acid) polyelectrolyte complex hydrogel. *Carbohydrate Research*, *345*, 1774–1780.
Tsao, C. T., Chang, C. H., Lin, Y. Y., Wu, M. F., Wang, J. L., Young, T. H., et al. (2011). Evaluation of chitosan/γ-poly(glutamic acid) polyelectrolyte complex for wound dressing materials. *Carbohydrate Polymers*, *84*, 812–819.
Ueno, H., Yamada, H., Tanaka, I., Kaba, N., Matsuura, M., Okumura, M., et al. (1999). Accelerating effects of chitosan for healing at early phase of experimental open wound in dogs. *Biomaterials*, *20*, 1407–1414.
Varga-Szabo, D., Braun, A., & Nieswandt, B. (2009). Calcium signaling in platelets. *Journal of Thrombosis and Haemostasis*, *7*, 1057–1066.
Wang, C. C., Su, C. H., Chen, J. P., & Chen, C. C. (2009). An enhancement on healing effect of wound dressing: Acrylic acid grafted and gamma-polyglutamic acid/chitosan immobilized polypropylene non-woven. *Materials Science and Engineering: C*, *29*, 1715–1724.
Xiao, C., Lachance, B., Sunahara, G., & Luong, J. H. T. (2002). Assessment of cytotoxicity using electric cell-substrate impedance sensing: Concentration and time response function approach. *Analytical Chemistry*, *74*, 5748–5753.
Xiao, C., & Luong, J. H. T. (2003). On-line monitoring of cell growth and cytotoxicity using electric cell-substrate impedance sensing (ECIS). *Biotechnology Progress*, *19*, 1000–1005.
Yates, C. C., Whaley, D., Babu, R., Zhang, J., Krishna, P., Beckman, E., et al. (2007). The effect of multifunctional polymer-based gels on wound healing in full thickness bacteria-contaminated mouse skin wound models. *Biomaterials*, *28*, 3977–3986.
Yu, D. G. (2007). Formation of colloidal silver nanoparticles stabilized by Na^+–poly(γ-glutamic acid)–silver nitrate complex via chemical reduction process. *Colloids and Surfaces B: Biointerfaces*, *59*, 171–178.